ELSEVIER
Catalysis Today 77 (2002) 3–16
CATALYSIS TODAY
www.elsevier.com/locate/cattod

Fuel processing for fuel cell systems in transportation and portable power applications[☆]

M. Krumpelt*, T.R. Krause, J.D. Carter, J.P. Kopasz, S. Ahmed

Electrochemical Technology Program, Chemical Technology Division, Argonne National Laboratory,
9700 S. Cass Avenue, Argonne, IL 60439, USA

Abstract

Small fuel cell systems in the 1–100 kW power range have become the focus of intense R&D activities. Applications envisioned for such systems include primary propulsion power for passenger cars and light-duty vehicles, auxiliary power for trucks and heavy-duty vehicles (for operator quality-of-life and housekeeping needs) and portable power generation for residential and recreational use. The operating mode of these small fuel cell systems differs dramatically from that of larger fuel cell systems (100–1000 kW) designed for utility power generation. These small systems will operate over a wide load range, with only brief periods at full power, considerable time at 30–50% of the rated power, and relatively frequent shutoffs and restarts. The lack of an infrastructure for producing and distributing H_2 has led to a research effort to develop on-board fuel processing technology for reforming hydrocarbon fuels to generate H_2. Existing reforming technology used in large-scale manufacturing operations, such as ammonia synthesis, is cost prohibitive when scaled down to the size of these small systems. Furthermore, these large reforming systems are designed to operate at a constant production rate and with infrequent shutoffs and restarts. In this paper, we provide an overview of the reforming options for generating H_2 from hydrocarbon fuels, the development of new reforming catalysts, and the design of fuel processors for these small fuel cell systems.

Keywords: Fuel cell systems; Portable power applications; Transportation; Fuel processing; Auto thermal reforming

1. Introduction

Fuel cell development has seen remarkable progress in the past decade because of an increasing need to improve energy efficiency as well as to address concerns about the environmental consequences of using fossil fuel for producing electricity and for propulsion of vehicles [1]. Because a fuel cell transforms chemical energy directly into electrical energy, its theoretical efficiency is not limited by the Carnot inefficiency problem for heat-to-work conversion, unlike conventional power generation plants and the internal combustion engine [2]. As a consequence, a fuel cell system can exhibit a higher fuel-to-electricity efficiency (generally 40–60% efficiency based on the lower heating value of the fuel) than almost all other energy conversion systems [3]. Fuel cell systems operating on pure H_2 produce only water, thus eliminating all emissions locally [1]. The emissions from a fuel cell system that

---

[☆] The submitted manuscript has been created by the University of Chicago as Operator of Argonne National Laboratory ("Argonne") under Contract No. W-31-109-ENG-38 with the US Department of Energy. The US Government retains for itself, and others acting on its behalf, a paid-up, nonexclusive, irrevocable world-wide license in said article to reproduce, prepare derivative works, distribute copies to the public, and perform publicly and display publicly, by or on behalf of the Government.

[*] Corresponding author. Tel.: +1-630-252-8520; fax: +1-630-252-4176.
E-mail address: krumpelt@cmt.anl.gov (M. Krumpelt).

0920-5861/02/$ – see front matter © 2002 Published by Elsevier Science B.V.
PII: S0920-5861(02)00230-4

operates using hydrocarbon fuels will be governed by the processing of the exhaust gases, which can be further combusted, reducing the emissions of CO and unburned hydrocarbons to trace levels [4].

Among the most successful applications of fuel cell technology has been in the US space program; 1 kW polymer electrolyte fuel cell (PEFC) systems, also known as polymer-exchange membrane fuel cells (PEMFC), were used in the Gemini program; 1 kW alkaline fuel cell (AFC) systems were used in the Apollo program; and 12 kW AFCs are used in the space shuttle program to generate electricity [1–3]. For power generation for small commercial and industrial buildings, a 200 kW phosphoric acid fuel cell (PAFC) system, the PC25^{TM}, has been developed by International Fuel Cells; more than 200 of these systems have been installed world-wide and have accumulated a total of 3.5 million operating hours [5]. Siemens Westinghouse has demonstrated a 100 kW solid oxide fuel cell (SOFC) cogeneration unit in The Netherlands (more than 14,000 operating hours) and a 25 kW SOFC unit in Japan (more than 13,000 operating hours). Siemens Westinghouse is planning to commercialize 250 and 1000 kW SOFC cogeneration systems and 300 and 1000 kW SOFC/gas turbine hybrid systems by 2004 [6].

Small fuel cell systems in the 1–100 kW power range have become the focus of intense research and development activities. Among the potential applications for fuel cells systems in this power range are primary propulsion for passenger and light-duty vehicles (50–100 kW), auxiliary power units (APUs) for operator quality-of-life and housekeeping needs for trucks and heavy-duty vehicles (2–10 kW), and portable power generation for residential and recreational needs (3–5 kW). The operating mode of these systems differs dramatically from that of larger fuel cell systems designed for utility power generation, which tend to operate at a relatively constant power output with infrequent shutoffs and restarts. These small systems will operate over a wide load range, with only brief periods at full power, considerable time at 30–50% of the rated power, and relatively frequent shutoffs and restarts. For transportation systems, the PEMFC is considered the leading fuel cell technology for primary propulsion [1,3,7–9]. The features of the PEMFC that make it attractive for transportation systems are its high power density and low operating temperature of 80 °C (important for rapid startup) and the fact that it is a solid system containing no free corrosive liquid, unlike the AFC. For auxiliary and portable power generation, both PEMFC and SOFC systems are being considered.

The lack of an infrastructure for producing and distributing H_2 has led to a research effort to develop on-board fuel processing technology for reforming hydrocarbon fuels to generate H_2 [1,7,9–11]. For transportation applications, the primary focus is on reforming gasoline, because a production and distribution infrastructure for gasoline already exists to supply internal combustion engines [12,13]. For APUs, the focus is on reforming both gasoline (for automotive applications [14]) and diesel (for trucks and heavy-duty vehicles [4]). For portable power generation, the focus has been on reforming natural gas for use in residential areas and liquefied petroleum gas for use in rural areas and for recreational use (e.g. camping). Existing reforming technology used in large-scale manufacturing processes, such as ammonia synthesis [15], is cost prohibitive when scaled down to the size of these small fuel cell systems (based on a typical cost-scaling coefficient of 0.6 for chemical process equipment). To be economically viable, small fuel cell systems cannot cost more than a few hundred dollars per kilowatt, in general, and they will have to cost less than US\$ 100 kW^{-1} for use in transportation systems. Furthermore, large commercial systems operate at a continuous production rate and are not designed to meet the varying power demands and frequent shutoffs and restarts of these small systems.

In this paper, we discuss the various options for reforming hydrocarbon fuels to generate H_2, the development of new reforming catalysts, and the design of fuel processors for these systems to meet cost and performance targets.

2. Reforming chemistry

The conversion of hydrocarbon fuels to H_2 can be carried out by several reaction processes, including steam reforming (SR), partial oxidation (PO), and autothermal reforming (ATR).

Steam reforming involves the reaction of steam with the fuel in the presence of a catalyst to produce H_2

and CO, as illustrated in Eq. (1) for methane, CH_4, and isooctane, C_8H_{18} (2,2,4-trimethylpentane, which is used as a surrogate for gasoline).

$$\begin{aligned} &CH_4 + H_2O \rightleftharpoons CO + 3H_2, \\ &\Delta H^\circ_{298} = +206.2\,\mathrm{kJ\,mol^{-1}} \\ &C_8H_{18} + 8H_2O \rightleftharpoons 8CO + 17H_2, \\ &\Delta H^\circ_{298} = +1273.2\,\mathrm{kJ\,mol^{-1}} \end{aligned} \tag{1}$$

In addition to H_2+CO, the fuel gas contains some CO_2 produced via the water–gas shift reaction (Eq. (2)).

$$CO + H_2 \rightleftharpoons CO_2 + H_2O \tag{2}$$

SR of light hydrocarbons, especially methane, is used for many large-scale manufacturing processes that require H_2, such as ammonia synthesis. Because SR is endothermic, in large-scale manufacturing processes the reaction is conducted in tube-fired furnaces at 800 °C and at pressures up to 30 atm [15]. The residence time is generally on the order of several seconds, for a gas-hourly space velocity (GHSV) of 2000–4000 h^{-1}. Coke produced by thermal cracking of hydrocarbons (Eq. (3)) or by the Bouduard reaction (Eq. (4)) leads to catalyst deactivation. These processes are problematic when the steam-to-carbon ratios are low, i.e. close to the stoichiometric ratio as defined in Eq. (1).

$$CH_4 \rightleftharpoons C + 2H_2, \qquad (CH_2)' \rightleftharpoons C + 2H_2 \tag{3}$$

$$2CO \rightleftharpoons C + CO_2 \tag{4}$$

To minimize coke formation excess steam is used to ensure that any carbon formed is gasified (Eq. (5)).

$$C + H_2O \rightleftharpoons CO + H_2 \tag{5}$$

For methane, a steam-to-carbon ratio of ~2.5 is sufficient to avoid coking. For higher hydrocarbons, a steam-to-carbon ratio of 6–10 is not uncommon [15]. Commercial catalysts consist of nickel supported on alumina, calcium aluminate, or magnesia. Rhodium catalysts are more active and less susceptible to coking than nickel catalysts but are more expensive [11].

Partial oxidation involves the reaction of oxygen with fuel to produce H_2 and CO when the oxygen-to-fuel ratio is less than that required for total combustion, i.e. complete conversion to CO_2 and H_2O (Eq. (6)).

$$\begin{aligned} &CH_4 + 0.5O_2 \rightleftharpoons CO + 2H_2, \\ &\Delta H^\circ_{298} = -35.7\,\mathrm{kJ\,mol^{-1}} \\ &C_8H_{18} + 4O_2 \rightleftharpoons 8CO + 9H_2, \\ &\Delta H^\circ_{298} = -158.1\,\mathrm{kJ\,mol^{-1}} \end{aligned} \tag{6}$$

The use of PO to generate H_2 (in particular synthesis gas [H_2 + CO]) for large-scale commercial applications has received some attention recently; however, such processes have not been extensively commercialized [16]. The reaction can be conducted with a catalyst (catalytic PO) or without a catalyst (non-catalytic PO). The reaction rates are much higher for PO than for SR, but the H_2 yield per carbon in the fuel is lower. For non-catalytic PO, reaction temperatures above 1000 °C are required to achieve rapid reaction rates. Although the reaction is exothermic, some of the fuel must be combusted, because the amount of heat generated by the reaction is not sufficient to preheat the feed to achieve optimal rates [15]. Recently, there has been an interest in catalytic PO, because it operates at a lower temperature than the non-catalytic route, thus providing better control over the reaction, minimizing coke formation, and allowing for a wider choice of materials of construction for the reactor. Catalysts are typically group VIII metals, such as rhodium, platinum, palladium, ruthenium, cobalt, nickel, and iridium, which are either supported on oxide substrates [17] or used unsupported, as metal wires and gauzes [18]. There is some debate on whether the reaction mechanism proceeds by a completely heterogeneous mechanism, i.e. one occurring only at the surface of the catalyst, or by a combination of a heterogeneous and a homogeneous mechanism, involving reactions both at the catalyst surface and in the gas phase [11]. Hickman and Schmidt [19–21], and Torniainen and Schmidt [22] have established that both the type of metal and the catalyst structure do influence the product distribution. There is also debate on whether H_2 and CO are primary reaction products or secondary reaction products. The latter view holds that complete oxidation of the hydrocarbon to generate CO_2 and H_2O occurs initially, followed by either steam or CO_2 reforming (or both) of the remaining hydrocarbons to generate H_2 and CO [11]. Schmidt has been focusing on short residence times of 10^{-2} to 10^{-4} s to minimize complete oxidation reactions [18].

Autothermal reforming involves the reaction of oxygen, steam, and fuel to produce H_2 and CO_2 (Eq. (7)).

$$\begin{aligned} &CH_4 + 0.5O_2 + H_2O \rightleftharpoons CO_2 + 3H_2, \\ &\Delta H^\circ_{298} = -18.4\,kJ\,mol^{-1} \\ &C_8H_{18} + 4O_2 + 8H_2O \rightleftharpoons 8CO_2 + 17H_2, \\ &\Delta H^\circ_{298} = -236.7\,kJ\,mol^{-1} \end{aligned} \tag{7}$$

In essence, this process can be viewed as a combination of PO and SR. The fuel gas contains a mixture H_2, CO_2, and CO, with the relative concentration being determined by the water–gas shift reaction (Eq. (2)) if thermodynamic equilibrium is achieved. ATR is not a new concept: it was used to produce town gas for use in many European communities in the early part of the 20th century [23]. No external heating source is required, because the exothermic oxidation reaction provides the heat necessary for the endothermic SR reaction. The oxidation reaction can be conducted with or without a catalyst, as previously discussed for PO, but most recent work has focused on catalytic oxidation.

3. Issues in selecting the appropriate reforming chemistry

The choice of the reaction process to be used for on-board reforming for small fuel cell systems depends on many factors, including the operating characteristics of the application (e.g. varying power demand, rapid startup, frequent shutdowns) and the type of fuel cell stack (e.g. PEMFC or SOFC). The US Department of Energy Office of Advanced Automotive Technologies (DOE/OAAT) has established long-range performance targets (to be met by fiscal year (FY) 2008) for a 50 kW fuel processor operating on Tier 2 gasoline for passenger and light-duty propulsion power. These targets include the ability to undergo multiple startups/shutdowns, achieve maximum power from a cold start (−20 °C) in 1 min, respond to changes in the power demand from 10 to 90% in 1 s, and have a power density of $800\,W\,l^{-1}$ [24]. SR is heat transfer limited and as such does not respond rapidly to changes in the power demand (i.e. “load following”). When power demand rapidly decreases, the catalyst can overheat, causing sintering, which in turn results in a loss of activity. ATR can overcome the load following limitations of SR, because the heat required for the endothermic reactions is generated within the catalyst bed, a property that allows for more rapid response to changing power demands and faster startup [25]. As discussed by Ahmed and Krumpelt [26], the lower operating temperature of catalytic ATR has a several advantages, for transportation applications, over the higher operating temperature of PO or the endothermic SR. Three advantages are particularly important: (1) less complicated reactor design and lower reactor weights, because less thermal integration (i.e. heat exchange between incoming reactants and the hot products) is required; (2) a wider choice of materials of construction; and (3) lower fuel consumption during startup because, for a given reactor mass, the energy required to heat a reformer to its operating temperature is proportional to its operating temperature. Although well-defined performance targets have not been established for fuel processors designed for use in APUs or portable power generation systems, the argument for also designing these fuel processors based on ATR are similar to those discussed above for automotive applications.

For ATR, Eq. (8) defines the idealized reaction stoichiometry for the production of H_2 from a carbonaceous fuel, where x is the oxygen-to-fuel molar ratio.

$$\begin{aligned} &C_nH_mO_p + x(O_2 + 3.7N_2) + (2n - 2x - p)H_2 \\ &\quad \rightarrow nCO_2 + (2n - 2x - p + (\tfrac{1}{2}m))H_2 + 3.7xN_2 \end{aligned} \tag{8}$$

In principle, the oxygen-to-carbon (O/C) and the steam-to-carbon (S/C) ratios can be chosen independently, as long as there is a surplus of O in the system sufficient to convert all of the C to CO_2. However, these ratios determine the energy released or adsorbed by the reaction, which defines the adiabatic reaction temperature and consequently, the concentration of H_2 in the fuel gas, as shown in Fig. 1 for isooctane. At the extreme value of an oxygen-to-isooctane ratio of 0, the relationship reduces to SR, with the highest percentage of H_2 (75.8%) in the fuel gas. At the other extreme value of an oxygen-to-fuel ratio of 12.5, the relationship reduces to complete combustion with a reaction temperature over 2000 °C with no H_2 being present in the fuel gas. At an oxygen-to-isooctane ratio of 2, the reaction is thermoneutral. It should be noted that percentage of H_2 in the fuel gas decreases as the

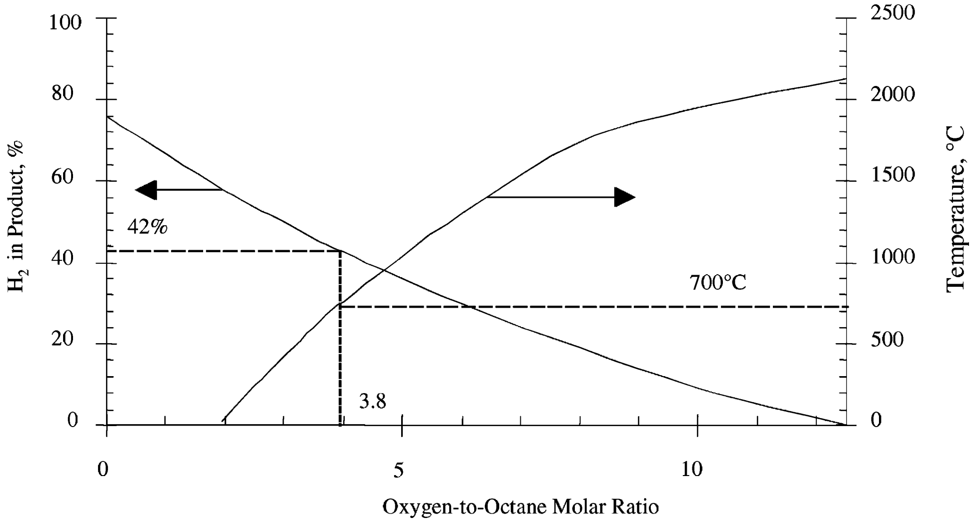

Fig. 1. The influence of the oxygen-to-isooctane molar ratio on the concentration of H_2 in the fuel gas and the adiabatic reaction temperature for ATR of isooctane (based on Eq. (8)).

oxygen-to-isooctane ratio increases not only because more H_2 is converted to H_2O, but also because of the dilution effect of N_2 (since air, and not pure oxygen, will be used as the oxidant in most applications).

For ATR, the maximum concentration of H_2 (35.5%) occurs at a temperature of ~700 °C, on the basis of thermodynamic equilibrium occurring when the oxygen-to-isooctane molar ratio is 4 (O/C = 1)

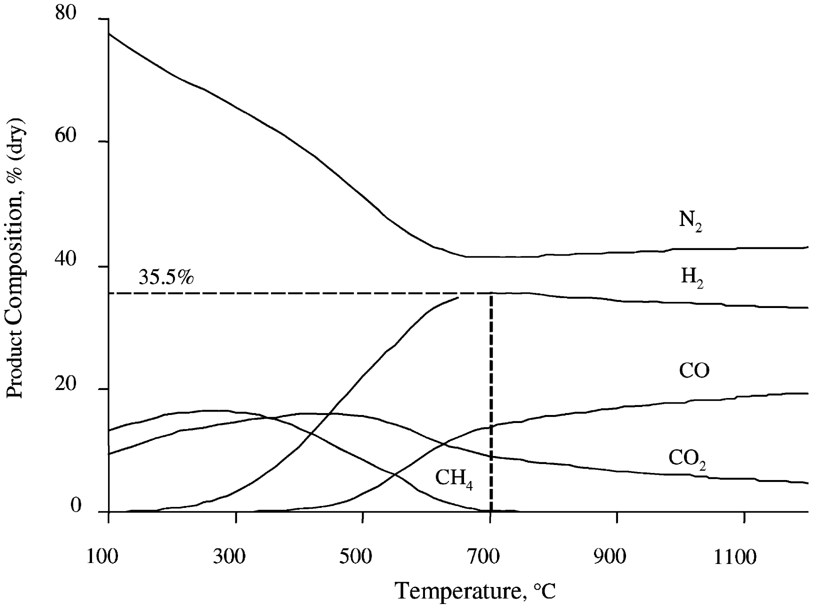

Fig. 2. Equilibrium gas composition for ATR of isooctane with an oxygen-to-isooctane ratio of 4 (O/C = 1) and a water-to-carbon ratio of 1 (H_2O/C = 1).

and the water-to-isooctane molar ratio is 1 ($H_2O/C = 1$), as shown in Fig. 2. Both the concentration of CO and CH_4 are relatively low at this temperature. As shown in Fig. 1, to achieve a reaction temperature of ∼700 °C requires an oxygen-to-isooctane molar ratio of ∼3.8. At a temperature >700 °C, the H_2 yield decreases due to the water–gas shift reaction (Eq. (3)) equilibrium, which favors the reactants ($CO + H_2O$). Because a PEMFC can not tolerate high CO concentrations, as will be discussed in the section on reactor design and engineering, the higher the concentration of CO in the fuel gas, the larger and heavier the fuel processor must be to process the fuel gas to reduce the CO concentration to acceptable levels.

4. Development of new reforming catalysts

The performance targets for the fuel processor for transportation fuel cell systems will require that the reforming catalysts used in these processors exhibit a higher activity and better thermal and mechanical stability than reforming catalysts currently used in the production of H_2 for large-scale manufacturing processes. To meet these targets, reforming catalysts will have to process the feed at a GHSV of 200,000 h^{-1} (based on the volumetric flow of the feed in the gaseous state at 25 °C and 1 atm) with a fuel conversion of >90% and a H_2 selectivity of >80% (moles of H_2 in product/moles of H_2 “extractable” from the feed), and have a lifetime of 5000 h [24]. Given the potential market for transportation applications, many of the major catalyst producers, such as Johnson-Matthey [27], Engelhard Corporation [28], dmc^2 division of OM Group Inc. [29] have begun to develop new reforming catalysts. At Argonne National Laboratory, we are developing new ATR catalysts based on SOFC technology, where a transition metal is supported on an oxide-ion-conducting substrate, such as ceria, zirconia, or lanthanum gallate, that has been doped with a small amount of a non-reducible element, such as gadolinium, samarium, or zirconium [30]. Süd-Chemie Inc., currently produces reforming catalysts based on this technology under a licensing agreement with Argonne.

Various transition metals supported on doped ceria have exhibited excellent reforming activity between 500 and 800 °C with high fuel conversion and high H_2 selectivity, as shown in Figs. 3 and 4, respectively. All metals investigated, except for Ag, exhibit a conversion of >95% at >600 °C, and all metals exhibited 100% conversion at >700 °C, as shown in Fig. 3. At <600 °C, conversion decreases more rapidly for first-row transition metals (in particular Ni and Co) than for second-row (Ru) and third-row (Pt, Pd) transition metals. The second- and third-row transition

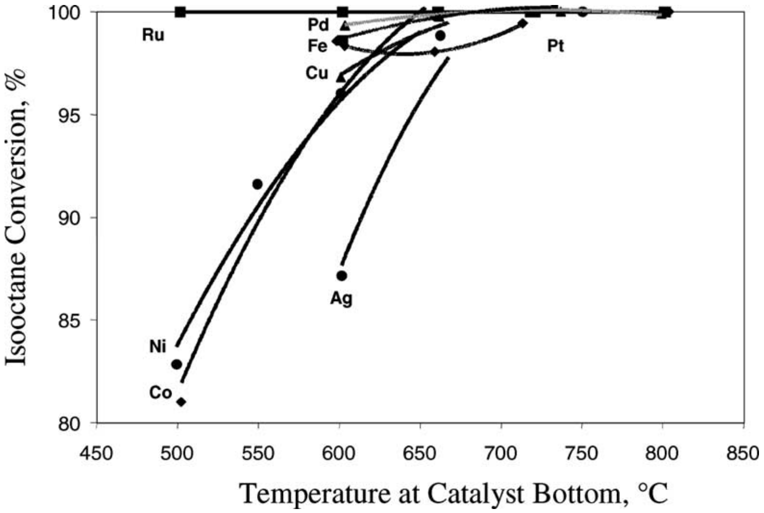

Fig. 3. Conversion of isooctane exhibited by various transition metals supported on doped ceria. Conditions: $O/C = 0.46$ (oxygen-to-isooctane molar ratio of 3.7), $H_2O/C = 1.14$, and GHSV =∼ 3000 h^{-1}.

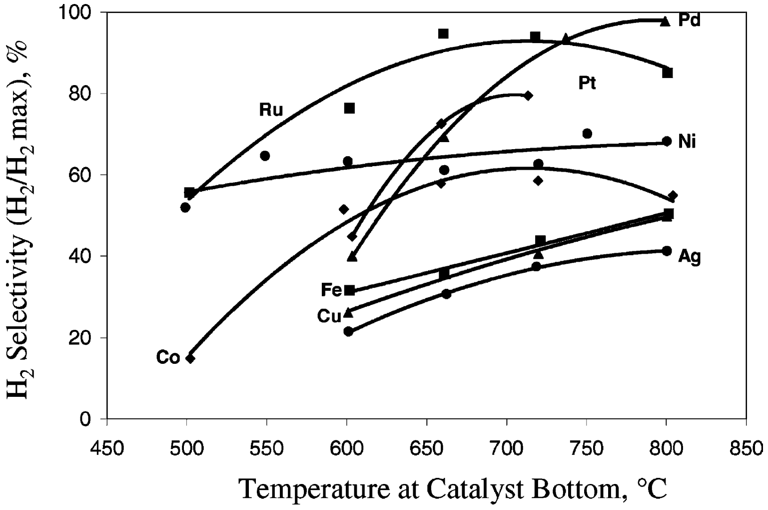

Fig. 4. Hydrogen selectivity exhibited by various transition metals supported on doped ceria. Conditions: O/C = 0.46 (oxygen-to-isooctane molar ratio of 3.7), $H_2O/C = 1.14$, and GHSV =~ 3000 h^{-1}.

metals exhibit a higher H_2 selectivity (>60%) than the first-row transition metals at >650 °C, as shown in Fig. 4. At temperatures <600 °C, the H_2 selectivity decreases to <50% for all metals, except for Ni and Ru.

Fig. 5 shows the yield for the primary reaction products (H_2, CO, CO_2, and CH_4) produced from reforming isooctane using Pt supported on doped ceria as a function of GHSV at 600 and 800 °C. Even at the highest GHSV investigated, some H_2 is present in the fuel gas (~4 mol H_2 per mole of isooctane observed at a GHSV of 150,000 at 600 °C and ~5.5 mol H_2 per mole of isooctane observed at a GHSV of 230,000 at 800 °C). At 600 °C, the H_2 yield remains constant at ~4 mol H_2 per mole of isooctane as the GHSV decreases from 150,000 to 75,000 h^{-1}. However, this yield then increases in a somewhat linear fashion as the GHSV further decreases from 75,000 to 15,000 h^{-1} with a yield of ~7.5 mol H_2 per mole of isooctane at 15,000 h^{-1}. At 800 °C, the H_2 yield increases in a somewhat linear fashion as the GHSV decreases over the entire GHSV range investigated, reaching a yield of ~9.5 mol H_2 per mole of isooctane in the feed at 15,000 h^{-1}. Although a mechanism has not been confirmed experimentally, it is suggested that the initial yield of H_2 observed at the highest GHSV investigated is produced by reactions of the fuel and O_2 and that both PO ($CO + H_2$) and total oxidation ($CO_2 + H_2O$) are occurring. Furthermore, these reactions involving fuel and O_2 are occurring at a time scale that is less than the contact time corresponding to the highest GHSV investigated (~15 ms). In the GHSV range investigated, steam and possibly CO_2 reforming are the predominant reactions responsible for the production of H_2.

In addition to reforming reactions that generate H_2, hydrocarbons fuels (except for CH_4) can undergo thermal cracking reactions to generate hydrocarbons with a lower carbon number than the parent hydrocarbons. For isooctane, small quantities of various hydrocarbons in the range of C_1–C_5 have been observed in the fuel gas produced at temperatures <650 °C using Pt supported on doped ceria [31]. Besides the products of thermal cracking, additional hydrocarbons, in particular CH_4, may be produced by the Fischer-Tropsch reaction. As shown in Fig. 5, CH_4 is observed in the fuel gas over the entire GHSV range investigated at both 600 and 800 °C. At 600 °C, the CH_4 yield decreases slightly as the GHSV decreases from 150,000 to 75,000 h^{-1}; the yield then increases slightly, going through a maximum, followed by a further decrease as the GHSV decreases from 75,000 to 15,000 h^{-1}. Thermal cracking of hydrocarbons may be responsible for the increase in the CH_4 yield, but this mechanism has not been verified experimentally. At 800 °C, CH_4 is the only hydrocarbon product observed in the

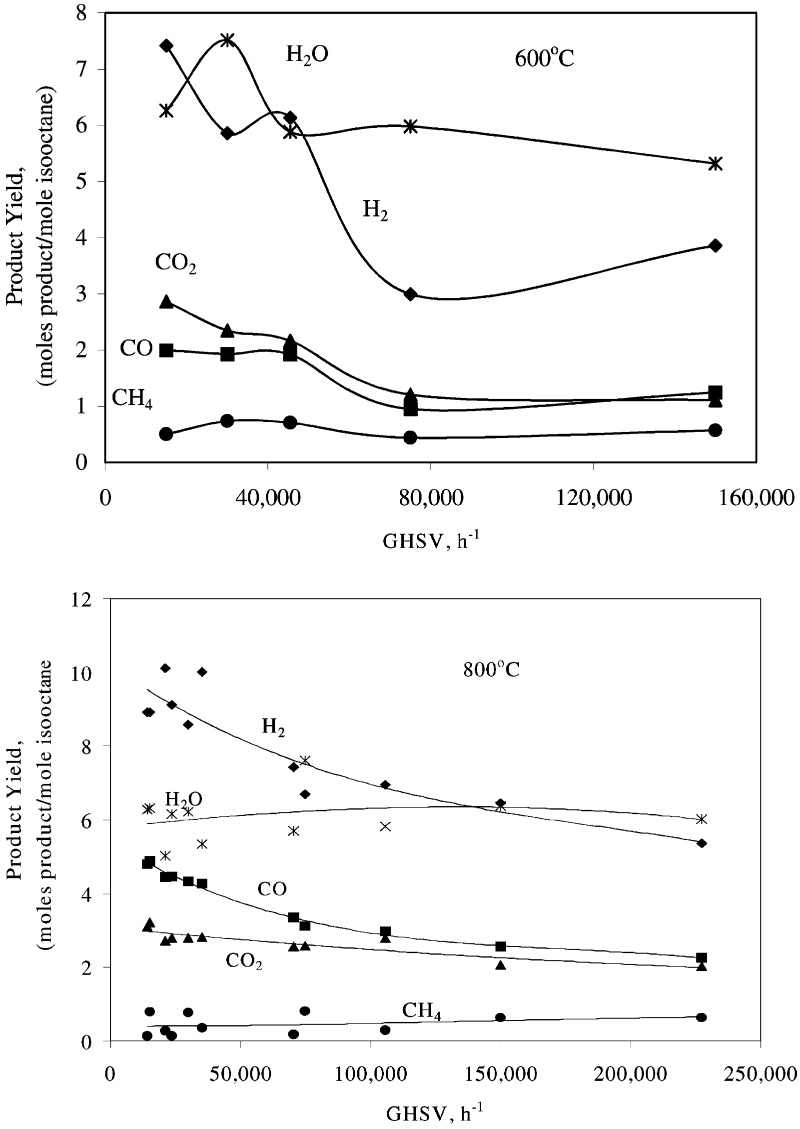

Fig. 5. Yield of primary reaction products (H_2, CO, CO_2, CH_4, and H_2O) as a function of GHSV for ATR of isooctane over Pt supported on doped ceria.

fuel gas, and its yield decreases slightly over the entire GHSV range investigated.

Sulfur tolerance is an important requirement for reforming catalysts because sulfur is present in most fuels being considered for generating H_2, e.g. natural gas, gasoline, and diesel. Fig. 6 shows that the percentage of H_2, CO, CO_2, and CH_4 in the fuel gas produced at 700 °C from reforming isooctane to which sulfur has been added in the form of benzothiophene. Sulfur concentrations ranged from 0 to 1300 ppm; the catalyst was Pt supported on doped ceria. The presence of sulfur did not appear to degrade the performance of this catalyst. In fact, there is a slight increase in the H_2 yield and a slight decrease in the CH_4 yield as the sulfur content of the fuel was increased from 0 to 100 ppm. For comparison, commercial nickel

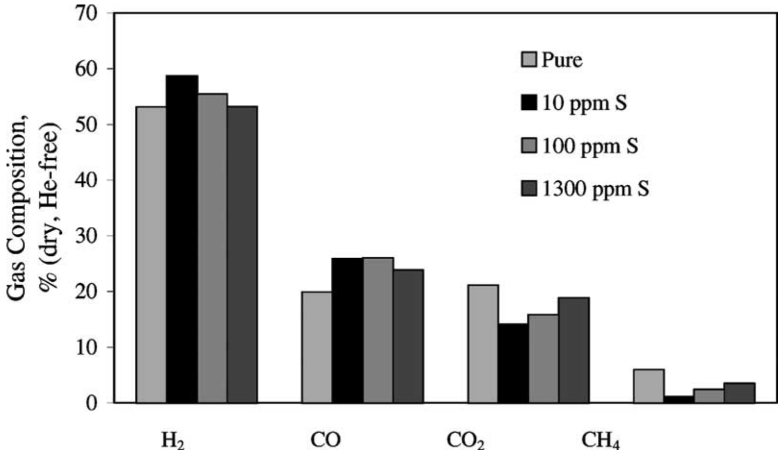

Fig. 6. Gas-phase composition (dry, He-free basis) produced from reforming isooctane containing sulfur concentrations ranging from 0 to 1300 ppm using Pt supported on a doped ceria. Sulfur was added as benzothiophene.

catalysts for SR show evidence of sulfur poisoning when the sulfur content of the gas is 50 ppm [15].

Common fuels, such as commercial-grade gasoline, are complex mixtures containing both aliphatic and aromatic compounds, in addition to additives, such as detergents, that improve engine performance and minimize engine wear. As shown in Fig. 7, Pt supported on doped ceria is capable of reforming a commercial-grade gasoline. The H_2 yield increases with increasing reaction temperature, approaching 60% (dry, He-free basis) at 750 °C. The theoretical H_2 yield is ∼68% for reforming isooctane, based on O/C = 0.5 and $H_2O/C = 1.1$ and assuming complete conversion of CO to CO_2.

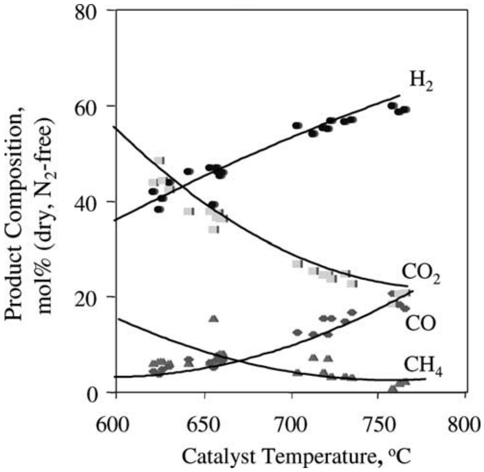

Fig. 7. Fuel gas composition as a function of temperature for reforming a commercial-grade gasoline using Pt supported on doped ceria.

5. Reformer design and engineering

As previously discussed, the design of the fuel processor depends on both the operating characteristics (e.g. the fuel, startup/shutoff frequency, and power demand) of the fuel cell system and on the ability of the fuel cell stack to tolerate reaction products, such as CO, and impurities in the fuel, such as sulfur.

The CO concentration is ∼10 mol% (dry basis) in the fuel gas generated from ATR of isooctane at 700 °C. At this high a concentration, CO poisons the PEMFC, because it is preferentially adsorbed by the Pt catalyst, thereby blocking the access of H_2 to these catalytic sites. The result is a significant reduction in the performance of the fuel cell stack. The CO concentration in the fuel gas must remain at or below 10 ppm for the PEMFC to maintain an acceptable level of performance [1,7,32,33]. The fuel processor for a PEMFC, therefore, must provide additional processing to reduce the CO concentration in the fuel gas exiting the reformer. In contrast, a SOFC can electrochemically oxidize CO to CO_2 to generate electric power without a significant decrease in performance [7]. The fuel processor for a SOFC system will not need to include any additional processing for CO.

The primary means of reducing the CO concentration in the fuel gas is the water–gas shift reaction (Eq. (3)). Based on thermodynamic equilibrium, the lower the reaction temperature, the lower the CO concentration that can be achieved [34]. For on-board fuel processing, the decrease in the catalytic rate as the reaction temperature decreases generally limits the CO concentration achievable by the shift reaction to 0.5–1 mol%. Two suitable catalysts are commercially available: an iron-chrome oxide catalyst, which operates at 300–450 °C, and a copper-zinc oxide catalyst, which operates at 160–270 °C. Industrially, the water–gas shift reaction is conducted using two or more reactor stages, which operate adiabatically based on the operating temperature regime of the catalyst used. For on-board fuel processing, there are two principal concerns: (1) the feasibility of keeping the iron-chrome and copper-oxide catalysts in the reduced state, especially during periods of shutdown; and (2) the pyrophoric nature of the copper-oxide catalyst in the reduced state. Because of these concerns, considerable R&D is being conducted to develop new water–gas shift catalysts for on-board fuel processing [35–38].

Various technologies have been investigated to reduce the concentration of CO in the fuel gas exiting the shift reactor to 10 ppm or less [1,7]. Among the candidates are membrane separation, methanation, and preferential CO oxidation (PrOX). For membrane separation, Pd alloy membranes can effectively remove the CO from the fuel gas, but such membranes require a large pressure difference and a high temperature that reduces system efficiency. For methanation, CO is reacted with H_2 to generate methane and water; however, the amount of H_2 required is three times the amount of the CO removed. For PrOX, a small quantity of air is bled into the fuel gas, and CO is selectively oxidized to CO_2 over the H_2 using a catalyst such as Rh or Ru supported on alumina. For on-board fuel processing, PrOX is the preferred method because of the lower parasitic system load and energy requirement compared to membrane separation and methanation [7].

Both the PEMFC and the SOFC are susceptible to sulfur poisoning, although sparse data are available showing the limiting concentration of H_2S in the fuel gas. For the PEMFC, irreversible loss of performance has been demonstrated at a H_2S concentration of 200 ppb [39]. For the SOFC system, a H_2S concentration of 1 ppm has been shown to cause virtually no degradation in cell performance [40]. In addition to the fuel cell stack, the reforming, water–gas shift, and PrOX catalysts may also be susceptible to sulfur poisoning.

Sulfur, primarily as H_2S, will be present in fuel gases produced from commercial-grade gasoline and diesel fuel, as well as from domestic, “pipeline” natural gas. New government standards will reduce the sulfur concentration in gasoline to an average of 30 ppm and a maximum of 80 ppm by 2006; however, fuel gas produced from these gasolines may contain as high as 3–8 ppm of H_2S [41]. Mercaptans added to domestic natural gas as an odorant for safety reasons will yield a fuel gas containing H_2S at a concentration on the order of that of the additive odorant in the feed gas.

Two different approaches are being investigated for removing sulfur in the fuel processor. In one approach, the fuel is desulfurized prior to being reformed by selectively adsorbing the organosulfur compounds in the fuel. International Fuel Cells has developed a Ni-based adsorbent reportedly capable of reducing the sulfur from the fuel without requiring the addition of steam or the recycling of H_2 [42]. In the second approach, the sulfur-containing fuel is first reformed and then the fuel gas is desulfurized by removing the H_2S using an oxide adsorbent, such as ZnO [41].

Fig. 8 illustrates the schematic of a fuel processing system for a PEMFC system. The major components of the system are (1) a catalytic reformer; (2) a shift reactor; (3) a PrOX reactor; (4) the fuel cell stack; (5) a turbo compressor to provide compressed air to the fuel cell stack, the reformer, and PrOX reactor; (6) a condenser/radiator to recover water; and (7) a water storage tank.

Fig. 9 illustrates the schematic of a fuel processing system for a SOFC system. The major components of the system are (1) a catalytic reformer; (2) the fuel cell stack; (3) a combustor/air preheater to preheat the air being fed to the cathode compartment; and (4) blowers for the air and anode gas recycle. Comparing Figs. 8 and 9, it is readily apparent that the fuel processing system for a SOFC is less complex than the system for a PEMFC, because the CO concentration does not have to be reduced in the SOFC system.

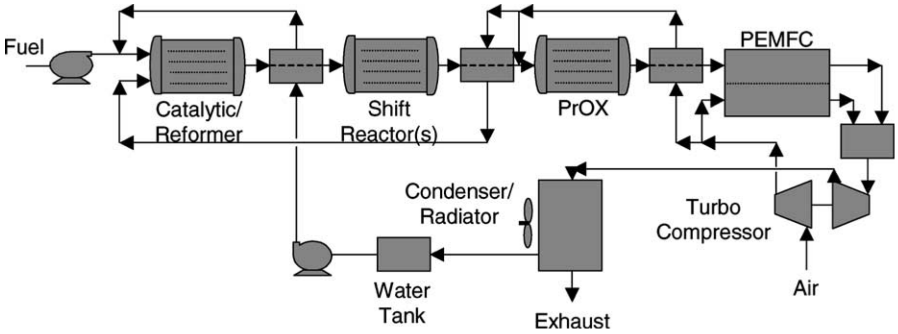

Fig. 8. Schematic of a fuel processing system for a PEMFC system.

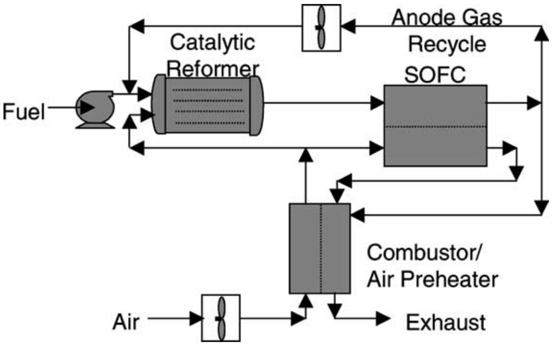

Fig. 9. Schematic of a fuel processor for a SOFC system.

Critical design issues for the fuel processor are minimizing gas-phase reactions, avoiding heat loss, and reducing thermal mass to facilitate rapid startup. These objectives have been approached by studying each of the unit operations, as shown in Figs. 8 and 9, individually. Various unit operations are then arranged into a single, integrated hardware enclosure, as shown schematically in Fig. 10, such that the desired flow rates, product concentrations, and temperature profiles are achieved within each functional component.

Gas-phase reactions can be minimized by ensuring that the reactants are delivered well-mixed and as close

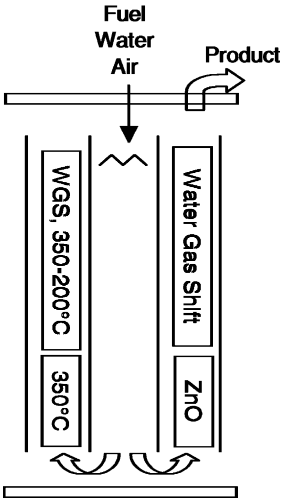

Fig. 10. Schematic of an integrated fuel processor system for a PEMFC system.

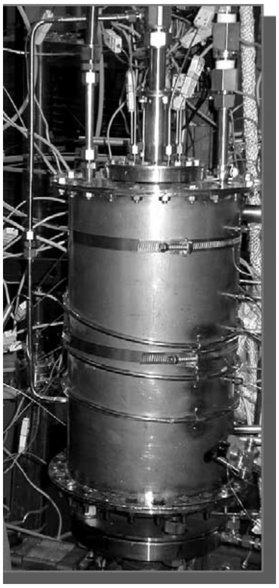

Fig. 11. The 10 kW integrated fuel processor based on ATR developed by Argonne National Laboratory.

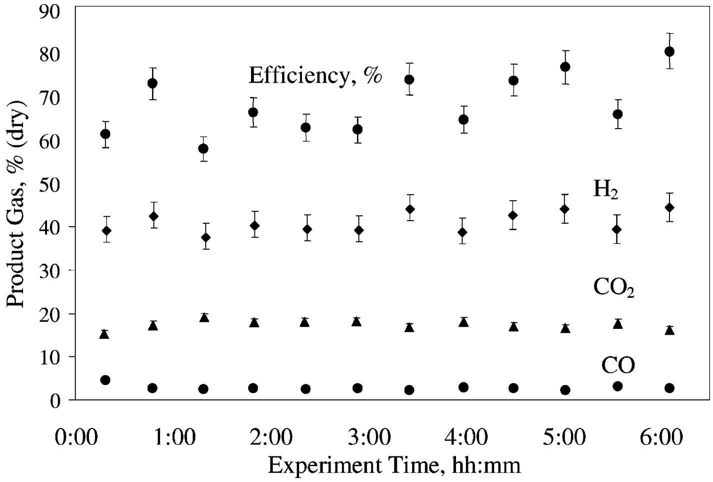

Fig. 12. Processor efficiency and fuel gas composition produced from reforming gasoline for the 10 kW integrated fuel processor.

to the surface of the reforming catalyst as possible, and by engineering the catalyst structure to minimize the void volume between catalytic surfaces. The structure of the catalyst (i.e. pellet or monolith) is important for reducing mass and heat transfer resistances and thus maintain a high overall reaction rate.

Rapid startup can be achieved by ATR because the heat necessary to rapidly heat the reactor can be generated by operating at a higher than normal oxygen-to-fuel ratio, i.e. so that more fuel is combusted. For practical applications, where a startup time on the order of 10 s is required, it is important that the reactor have a low thermal mass. For a given reactor mass, the energy required to heat the processor to its operating temperature is proportional to its operating temperature. Rapid startup can be achieved by operating at low temperatures and by reducing the weight of the hardware—including the catalyst, the heat exchange surfaces, and the required insulation.

We have developed a 10 kW integrated fuel processor for use with a PEMFC system, shown in Fig. 11. The reactor has a volume of 13 l, resulting in a power density of 0.77 kW l^{-1}. As shown in Fig. 12, the processor is capable of reforming gasoline to produce a fuel gas containing approximately 40 mol% H_2 (dry basis) with efficiencies in the high 70% range. The reactor is capable of producing a fuel gas containing ~25% H_2 at 25% of full power within 15 min of startup, as shown in Fig. 13. Further development is focused on reducing the startup time to 1 min or less.

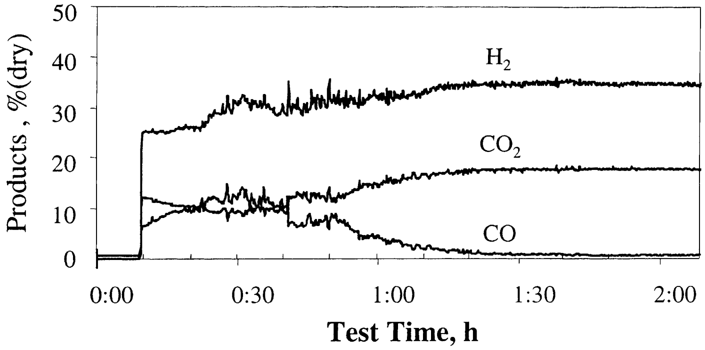

Fig. 13. Fuel gas composition during startup of the 10 kW integrated fuel processor.

6. Summary

A new generation of fuel processors based on ATR and specially designed for small fuel cell systems is emerging. These new reactors have a power density of almost 1 kW l^{-1}, can be started rapidly and can follow load variations with ease. The efficiency of these new reactors is close to the theoretical limit. New types of catalysts are showing promise to support the PO chemistry of the fuel reforming reactions. Commercialization of such processes is expected within 1–2 years.

Acknowledgements

The authors would like to acknowledge Candido Pereira and Sheldon Lee, who provided data on performance data on the 10 kW integrated fuel processor, and Rolf Wilkenhoener, who performed the experimental work on the reforming activity of the various transition metals on a doped-ceria support. This work was supported by the US Department of Energy, Office of Transportation Technologies, Office of Advanced Automotive Technologies, under Contract No. W-31-109-ENG-38.

References

[1] L. Carrette, K.A. Friedrich, U. Stimming, Fuel Cells 1 (2001) 5.
[2] A.J. Appleby, in: J.J. McKetta, W.A. Cunningham (Eds.), Encyclopedia of Chemical Processing and Design, vol. 24, Marcel Dekker, New York, 1986, p. 1.
[3] K. Kinoshita, E.J. Cairns, in: J. Kroschwitz, M. Howe-Grant (Eds.), Kirk-Othmer Encyclopedia of Chemical Technology, 4th ed., vol. 11, Wiley, New York, 1994, p. 1098.
[4] H.H. Dobbs Jr., T. Krause, R. Kumar, M. Krumpelt, in: A.J. McEvoy (Ed.), Proceedings of the 4th European Solid Oxide Fuel Cell Forum, Lucerne, Switzerland, 10–14 July 2000, p. 85.
[5] International Fuel Cells, http://www.ifc/whoweare/milestones.shtml.
[6] Siemens Westinghouse, http://www.siemenswestinghouse.com/en/fuelcells/history/index.cfm.
[7] J.H. Hirschenhofer, D.B. Staufer, R.R. Engleman, M.G. Klett, Fuel Cell Handbook, 4th ed., US Department of Energy, DOE/FETC-99/0176, 1999.
[8] T.R. Ralph, G.A. Hards, Chem. Ind. (1998) 337.
[9] V. Ranabm, Chem. Ind. (1997) 771.
[10] S. Golunski, Platinum Metals Rev. 42 (1998) 2.
[11] D.L. Trimm, Z.I. Õnsan, Catal. Rev.-Sci. Eng. 43 (2001) 31.
[12] Arthur D. Little Inc., Multifuel Reformers for Fuel Cells Used in Transportation—Assessment of Hydrogen Storage Technologies, US Department of Energy, DOE/CE/50343-1, 1994.
[13] R.L. Espino, J.L. Robbins, Fuel and fuel reforming options for fuel cell vehicles, in: Proceedings of the 30th International Symposium on Automotive Technology and Automation, Florence, Italy, 16–19 June 1997.
[14] Delphi Automotive Systems, http://www.delphiauto.com/news/pressReleases/pr439-02162001.
[15] L.D. Pesce, W.R. Jenks, in: J.A. Kent (Ed.), Riegel's Handbook of Industrial Chemistry, 9th ed., Van Nostrand Reinhold, New York, 1992, p. 1068.
[16] S.S. Bharadwaj, L.D. Schmidt, Fuel Process. Technol. 42 (1995) 109.
[17] K.H. Hofstad, J.H.B.J. Hoebink, A. Holmen, G.B. Marin, Catal. Today 40 (1998) 157.
[18] L.D. Schmidt, in: A. Corma, F.V. Melo, S. Mendioroz, J.L.G. Fierro (Eds.), Studies, Elsevier, Amsterdam, Surf. Sci. Catal. 130 (2000) 61.
[19] D.A. Hickman, L.D. Schmidt, J. Catal. 138 (1992) 267.
[20] D.A. Hickman, L.D. Schmidt, Catal. Lett. 17 (1993) 223.
[21] D.A. Hickman, L.D. Schmidt, Science 259 (1993) 343.
[22] P. Torniainen, L.D. Schmidt, J. Catal. 146 (1994) 1.
[23] M. Flytzani-Stephanopoulos, G.E. Voecks, J. Hydrogen Energy 8 (1983) 539.
[24] US Department of Energy, Office of Transportation Technologies, 2001 Annual Progress Report, p. 1.
[25] R. Kumar, S. Ahmed, M. Krumpelt, K.M. Myles, US Patent 5,248,566 (1993).
[26] S. Ahmed, M. Krumpelt, Int. J. Hydrogen Energy 26 (2001) 291.
[27] Johnson-Matthey, http://www.johnsonmatthey.com.
[28] R.J. Farrauto, The catalytic generation of hydrogen for the solid polymer membrane fuel cell, in: Proceedings of the 17th North American Catalysis Society Meeting, Toronto, Canada, 3–8 June 2001.
[29] S. Wieland, F. Baumann, K. Starz, in: Proceedings of the Extended Abstracts on Fuel Cell Seminar 2000, Portland, Oregon, 30 October–2 November 2000, p. 309.
[30] M. Krumpelt, S. Ahmed, R. Kumar, R. Doshi, US Patent 6,110,861 (2000).
[31] M. Krumpelt, T. Krause, J.D. Carter, J. Mawdsley, J.-M. Bae, S. Ahmed, C. Rossignol, Catalytic autothermal reforming, in: Proceedings of the Annual National Laboratory R&D Meeting, DOE Fuel Cells for Transportation Program, Oak Ridge, Tennessee, 6–8 June 2001.
[32] S. Gottesfeld, Polymer electrolyte fuel cells: potential transportation and stationary applications, in: Proceedings of the EPRI/GRI Fuel Cell Workshop on Technology Research and Development, New Orleans, Louisiana, 12–14 April 1993.
[33] International Fuel Cells, Investigation of Design and Manufacturing Methods for Low-Cost Fabrication of High Efficiency, High Power Density PEM Fuel Cell Power Plant, Final Report FCR-11320A, South Windsor, Connecticut, 10 June 1991.
[34] D.S. Newsome, Catal. Rev.-Sci. Eng. 22 (1980) 273.

[35] S. Swartz, C. Holt, W. Dawson, in: Proceedings of the Extended Abstracts on Fuel Cell Seminar 2000, Portland, Oregon, 30 October–2 November 2000, p. 298.

[36] J. Patt, C. Phillips, D. Moon, L.T. Thompson, Catal. Lett. 65 (2000) 193.

[37] S. Hillaire, X. Wang, R.J. Gorte, J. Wagner, Appl. Catal. A 215 (2001) 271.

[38] D.J. Myers, J.F. Krebs, T.R. Krause, J.D. Carter, Prep. Symp. Catal. Fuel Chem. 46 (2001) 676.

[39] T. Zawodzinski, F. Uribe, W. Smith, T. Springer, J. Valerio, D. Vernon, T. Rockward, D. McMurry, G. Bender, M. Hickner, E. Brosha, B. Orler, C. Adams, R&D on optimized cell performance for operation on reformate and air, in: Proceedings of the Annual National Laboratory R&D Meeting, DOE Fuel Cells for Transportation Program, Oak Ridge, Tennessee, 6–8 June 2001.

[40] N. Maskalick, Contaminant effects in solid oxide fuel cells, in: Proceedings of the Fourth Annual Fuel Cells Contractors Review Meeting, US DOE/METC, July 1992.

[41] J.D. Carter, T. Krause, J. Mawdsley, R. Kumar, M. Krumpelt, Sulfur removal from reformate, in: Proceedings of the Annual National Laboratory R&D Meeting, DOE Fuel Cells for Transportation Program, Oak Ridge, Tennessee, 6–8 June 2001.

[42] L.J. Bonville, C.L. DeGeorge, P.F. Foley, J. Garow, R.R. Lesieur, J.L. Preston, D.F. Szydlowski, US Patent 6,159,256 (2000).